

Reactions of 1, ω -bis(2-bromopyridinium)alkanes with hydroxide ion in aqueous solutions

Carmen Fernandez,¹ Vicente G. Toscano,² Hernan Chaimovich,¹ Mario J. Politi^{1*} and Noboru Hioka³

¹Departamento de Bioquímica, Instituto de Química da Universidade de São Paulo, São Paulo, SP, Brazil

²Departamento de Química Fundamental, Instituto de Química da Universidade de São Paulo, São Paulo, SP, Brazil

³Departamento de Química, Fundação Universidade de Maringá, Maringá, Pr, Brazil

Received 18 September 1996; revised 17 February 1997; accepted 18 April 1997

ABSTRACT: The reaction of OH⁻ ion with 1, ω -bis(2-bromopyridinium)alkanes, where the reaction centers are separated by a varying number of methylene groups, was investigated to model the increased velocity of OH⁻ attack on pre-micellar aggregated *N*-alkylpyridinium compounds. 1, ω -Bis(2-bromopyridinium)alkanes (RPBr) [R = propane (I), butane (II), pentane (III), hexane (IV) and octane (V)] were synthesized and characterized by standard procedures. The kinetics of I–V with OH⁻ ion fitted two consecutive first-order reactions. The intermediate products, 1-(2-pyridone)- ω -(2-bromopyridinium)alkane, and also the final products 1, ω -bis(2-pyridone)alkanes, were isolated. Deuterium isotope effects, activation parameters and salt effects on the reaction rates suggest that OH⁻ attack is rate limiting and there is a through-space acceleration of the initial attack due to the proximity of the positive charges. These results place an upper limit of 20-fold for the electrostatic acceleration in OH⁻ attack in pre-micellar aggregates. © 1998 John Wiley & Sons, Ltd.

KEYWORDS: 1, ω -bis(2-bromopyridinium)alkanes; hydroxide ion

INTRODUCTION

Reactions of OH⁻ with 4-cyano-*N*-alkylpyridinium ions (RPCN) produce the corresponding pyridones (P) and amides (A), by nucleophilic attack at either the CN group or at C-4 of the pyridinium ring.^{1,2} For a series of RCPNs, with R varying from methyl to dodecyl, the first-order rate constants for alkaline hydrolysis (k_{ψ}), in excess OH⁻, are independent of RPCN concentration up to 1×10^{-3} M substrate.² For 4-cyano-*N*-hexadecylpyridinium (HPCN), however, the values of k_{ψ} and the P/A ratios increase with [HPCN] from concentrations as low as 1×10^{-6} M.² HPCN is a detergent and its critical micelle concentration (CMC), measured by conductivity or fluorescence quenching, is *ca* 1×10^{-3} M, well above the concentration where the reaction rate and products for OH⁻ ion attack change with concentration.² HPCN, and also other RPCNs with R > butyl, are incorporated in hexadecyltrimethylammonium halide (HTAX) micelles.^{2,3} The reaction rate of micellar-incorporated RPCN with OH⁻ is orders of magnitude faster than the reaction in aqueous solution.^{2,3} As for many other bimolecular reactions, the calculated second-order rate constant in the micelle is

only 10 times higher than that in water.⁴ The reaction product in the micelle, however, is exclusively pyridone.² In view of the above, we postulated that rate increase, and preferred formation of pyridone observed for the reaction of HPCN with OH⁻ below the CMC, are due to the formation of pre-micellar aggregates of HPCN.²

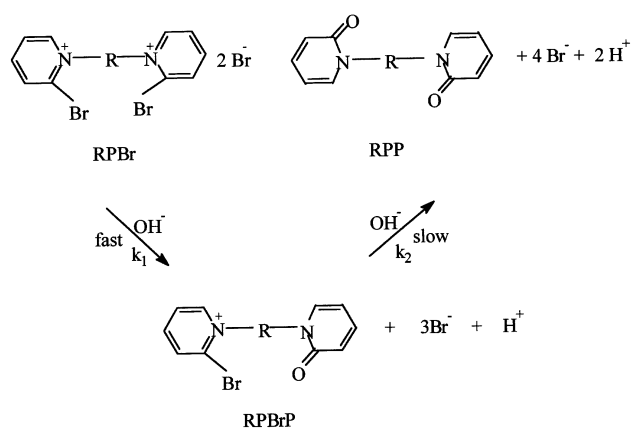
Aggregation often modifies, sometimes profoundly, the mechanism or rate of thermal reactions.^{5–12} In a supramolecular aggregate, such as a micelle formed by a positively charged substrate, rate increases for reactions with negatively charged ions (counterions), such as OH⁻, arises from hydroxide ion concentration at the interface.^{11,12} Surface electrostatic effects may also modify the relative energy of initial and transition states in the surface of micelles.^{12,13} Below the CMC, however, the size of aggregates is a matter of debate, although in some systems detergent dimers have been demonstrated.^{2,14–19} Investigation of reaction rates in a detergent dimer should contribute to our understanding of kinetic effects observed in the pre-micellar region. However, the results are difficult to interpret because the distribution of aggregated species is unknown, and in dynamic equilibrium, and the isolation of kinetic contributions of a unique aggregate demands numerous assumptions and complex fitting procedures.

A simple model for a detergent dimer is a molecule containing reactive groups linked by methylene spacers of different lengths. Hydroxide ion attack on biscyano-pyridiniums produces two intermediates and at least three

*Correspondence to: M. J. Politi, Departamento de Bioquímica, Instituto de Química da Universidade de São Paulo, São Paulo, SP, Brazil.

E-mail: mjpoliti@usp.br

Contract/grant sponsor: CNPq; Contract/grant sponsor: FAPESP; Contract/grant sponsor: CAPES; Contract/grant sponsor: FINEP.



products; hence, to focus attention on the effect of the distance between the two positive centers of the dimer on the reaction rate, it is desirable to examine the reactivity of compounds exhibiting simpler reaction pathways. The reaction of 2-bromo-*N*-alkylpyridiniums with OH^- produces solely (the corresponding) 2-pyridone.²⁰ In the present study, we examined the reaction of OH^- ion with a series of 1, ω -(2-bromopyridinium)alkanes (RPBr)

and investigated the effect of the distance between the pyridinium groups on reaction rates.

EXPERIMENTAL

Acetonitrile, 2-bromopyridine, 1,3-dibromopropane, 1,4-dibromobutane, 1,5-dibromopentane, 1,6-dibromohexane and 1,8-dibromooctane (Aldrich) were distilled before use. All other reagents were of analytical grade or better. Deionized, doubly glass-distilled water was used throughout.

The bis(2-bromopyridinium)alkanes were synthesized from the reaction of 2-bromopyridine with the corresponding dibromoalkane.²¹ The reflux times were 13 h for 1,3-bis(2-bromopyridinium)propane dibromide (**I**), 14 h for 1,4-bis(2-bromopyridinium)butane dibromide (**II**), 20 h for 1,5-bis(2-bromopyridinium)pentane dibromide (**III**), 60 h for 1,6-bis(2-bromopyridinium)hexane dibromide (**IV**) and 120 h for 1,8-(2-bromopyridinium)octane dibromide (**V**). The products were recrystallized twice from ethanol and vacuum dried at room temperature. Melting points ($^{\circ}\text{C}$) and elemental analyses (%) were as follows: **I**, m.p. 239–241, C, H, N exp. 28.19, 3.25, 5.05 and found 28.73, 3.08, 4.03; **II**, m.p. 256–258,

Table 1. UV, ^1H NMR and ^{13}C NMR of RPBR, bispyridones (RPP) and of the intermediate compound (RPBrP) for R = propane (**XI**)

Compound	λ_{max} (nm) ^a (ϵ , $\text{l mol}^{-1} \text{cm}^{-1}$)	^1H NMR ^b	^{13}C NMR ^b
RPBr (I)	277 (16 000)	2.47–2.63 (q, 2H) 4.81 (t, 4H) 7.83–7.93 (m, 2H) 8.22 (d, 4H) 8.88 (d, 2H)	28.65, 58.75 127.23, 134.71 138.24, 146.71 147.31
RPP (VI)	296 (11 200)	1.67–1.78 (m, 2H) 3.64 (t, 4H) 6.11–6.22 (m, 4H) 7.18–7.26 (m, 4H)	27.63, 47.15 109.06, 118.71 138.26, 141.81 163.35
RPBr (V)	277.5 (15 600)	1.11 (m, 8H) 1.69–1.76 (m, 4H) 4.5 (t, 4H) 7.7–7.78 (m, 2H) 8.07 (d, 4H) 8.71 (d, 2H)	25.0, 27.56 28.77, 62.94 126.75, 134.41 137.76, 145.82 147.02
RPP (X)	296 (11 000)	3.31 (m, 4H) 4.24 (m, 4H) 4.67 (m, 4H) 6.96 (t, 4H) 9.5–9.62 (m, 4H) 10.63–10.66 (m, 4H)	24.93, 27.56 27.88, 50.09 109.01, 118.55 138.84, 141.76 163.64
RPBrP (XI)	277 (8000) 296 (5600)	1.82 (q, 1H) 2.02 (q, 1H) 3.02–4.13 (m, 4H) 6.14–6.24 (m, 3H) 7.07–7.36 (m, 4H) 8.01–8.08 (m, 1H)	27.41, 28.34 47.27, 59.67 109.39, 118.95 127.05, 134.51 138.39, 141.94 142.24, 146.29 146.89, 164.48

^a λ_{max} = absorption wavelength maxima.

^b Chemical shifts in ppm using TMS as the standard.

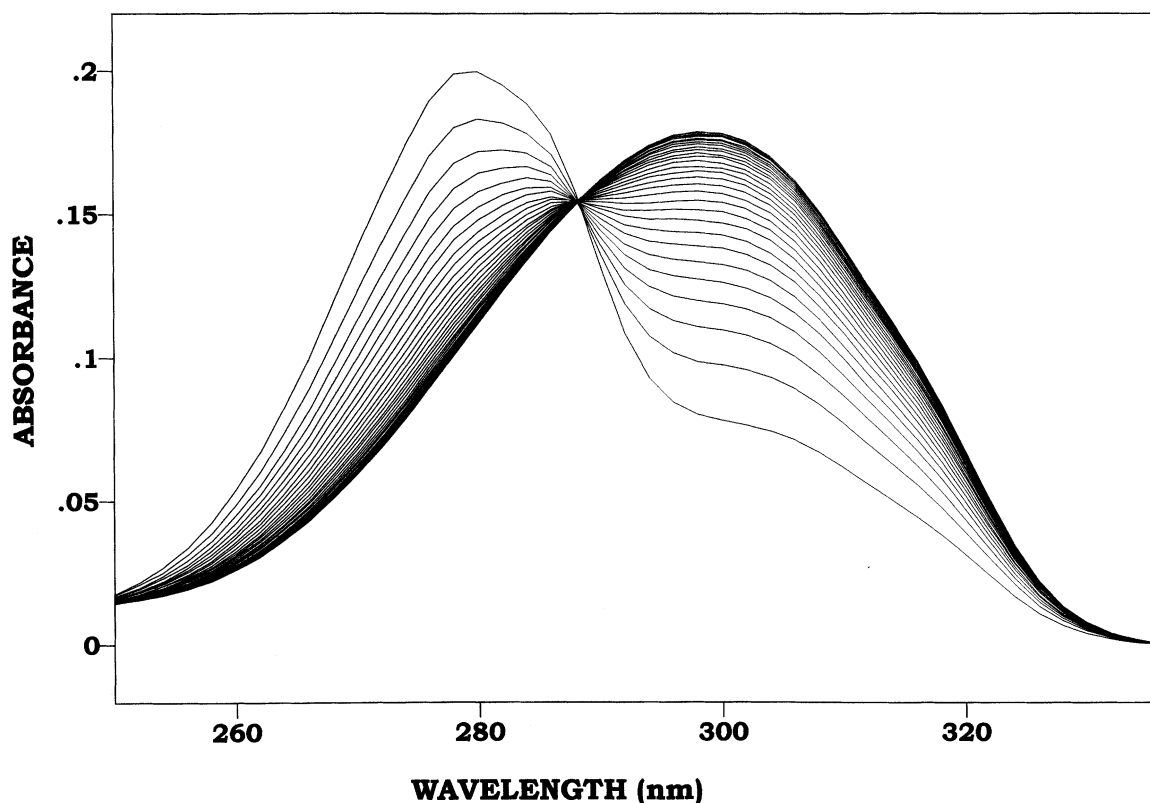


Figure 1. Spectral time dependence for the alkaline hydrolysis of 1,3-bis(2-bromopyridinium) propane dibromide (**I**). Conditions: $[\text{NaOH}] = 5 \times 10^{-3} \text{ M}$; $[\text{I}] = 2 \times 10^{-5} \text{ M}$; temperature = 25°C . The time between the scans is 30 s

C, H, N exp. 31.61, 3.03, 5.26 and found 30.86, 3.1, 4.88; **III**, m.p. 207–209, C, H, N exp. 33.00, 3.32, 5.13 and found 32.74, 3.36, 4.56; **IV**, m.p. 232–233, C, H, N exp. 34.32, 3.60, 5.00 and found 34.44, 3.49, 4.78; **V**, m.p. 178–180, C, H, N exp. 36.77, 4.11, 4.76 and found 35.91, 4.14, 4.49. The results of bromide titration²² were within experimental error. Proton and carbon NMR spectra were in accord with the structure.²³ For **I–V** the molar absorbances of the pyridinium substrates at 277 and 296 nm were $16\,000 \pm 150$ and 400 ± 100 , respectively.²³

The reaction products, isolated after complete reaction of **I–V** with OH^- , were isolated and characterized by ^1H and ^{13}C NMR and UV spectrometry. All data were consistent with the formation of the expected bispyridone (Scheme 1).²⁰

The intermediate 1-(2-pyridone)-3-(bromopyridinium)propane (**XI**) was isolated in good yield from a reaction mixture containing **I**. Aliquots of a reaction mixture of **I** and OH^- , withdrawn at convenient times, were acidified with 5 M acid and separated by thin-layer chromatography (TLC) (0.5 M NaBr in methanol).^{23,24} Compound **XI** was isolated by preparative TLC of a scaled-up reaction mixture. The ^1H and ^{13}C NMR (D_2O) and UV spectra were consistent with the structure shown in Scheme 1. The multiplets between $\delta 1.82$ and 2.02 were

assigned to the central methylene group of **XI** (Table 1). The deshielding of the pyridinium protons indicates partial stabilization of the positive charge of the ring. This effect can be attributed to a conformation in which both rings are in proximity. Preliminary energy minimization calculations suggest the existence of a local minimum where both rings are in proximity, as opposed to RPBBr where the central chain is fully extended. The NMR data are in full agreement with the proposed structure.

Reaction kinetics were followed at 296 nm in excess OH^- at 25°C in a Beckman Model 70 spectrophotometer.

RESULTS AND DISCUSSION

The final products from the reaction of **I** and **V** with OH^- ion, isolated in 90% yield from scaled-up reaction mixtures, were the corresponding 1, ω -bis(2-pyridone)-alkanes (Scheme 1). The UV and NMR spectra of 1,3-bis(2-pyridone)propane (**VI**) and 1,8-bis(2-pyridone)-octane (**X**) were consistent with the proposed structures (Table 1).²³ The final products from the reaction of **II–IV** with OH^- were not isolated, but the UV spectra were those expected (not shown).

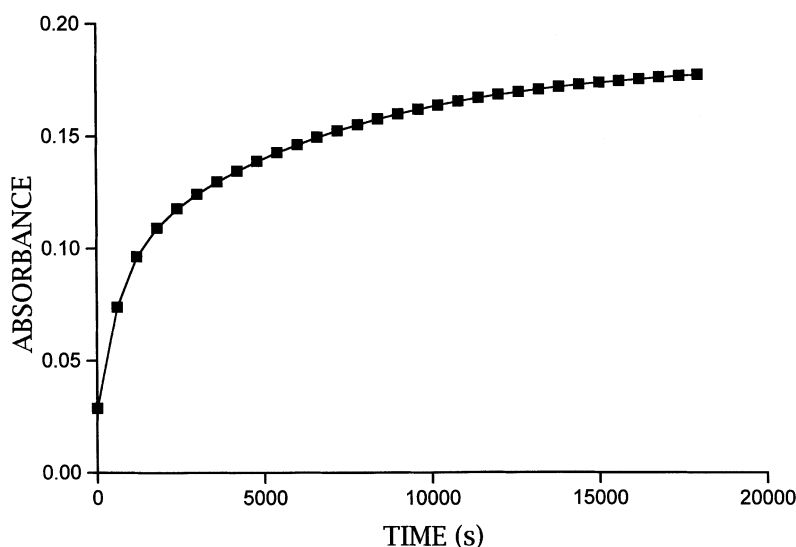


Figure 2. Experimental and simulation absorbance changes ($\lambda = 296$ nm) for the alkaline hydrolysis of 1,3-bis(2-bromopyridinium) propane dibromide (I). Conditions: (■) experimental, hydrogencarbonate buffer concentration = 20 mM, pH = 10.3, $[I] = 1.7 \times 10^{-5}$ M; (solid line) simulation, $[I] = 1.7 \times 10^{-5}$ M, $k_1 = 1.5 \times 10^{-3} \text{ s}^{-1}$, $k_2 = 1.5 \times 10^{-4} \text{ s}^{-1}$, $P = 0.1834$, $Q = 0.092$, $R = -0.062$ [see equation (1)]

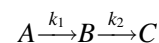
The kinetics of the reaction of I–V with OH^- ion, exemplified in Fig. 1 was followed spectrophotometrically. The spectra of the reaction mixture of compounds I–V with OH^- exhibited an isosbestic point at 288 nm (Fig. 1). First-order analysis of the change in absorbance (at 277 or 296 nm) with time did not fit the experimental data. The variation of absorbance (Abs) with time (t) fitted the following equation (Fig. 2):

$$\text{Abs} = P - Q \exp(-Ft) + R \exp(-Gt) \quad (1)$$

where P , Q , F , R , and G are the fitting parameters.

Several two-step reaction pathways yield kinetic fits to equation (1).²⁵ One particular reaction pathway, fast OH^- attack on RPBr yielding a half-reacted pyridone, followed by a slower OH^- attack on the intermediate, is consistent with both the kinetic and structural data for this reaction.

This reaction pathway can be represented as²⁵



where, A, B and C are the initial RPBr, intermediate product and final pyridone, respectively (Scheme 1). In

Table 2. Rate constants for the reaction of compounds I–V with OH^- ion

pH	k ($\text{s}^{-1} \times 10^3$) ^a	I	II	III	IV	V
10.3	k_1	1.74	0.74	0.47	0.27	0.16
	k_2	0.19	0.12	0.1	0.07	0.05
10.6	k_1	2.85	0.97	0.56	0.44	0.26
	k_2	0.33	0.19	0.14	0.13	0.09
11.0	k_1	6.27	2.35	1.37	1.00	0.72
	k_2	0.74	0.47	0.37	0.32	0.27
11.3	k_1	11.3	4.15	2.22	1.79	1.07
	k_2	1.47	0.85	0.65	0.58	0.47
11.8	k_1	47.3	17.6	10.3	6.90	4.02
	k_2	4.9	3.01	2.22	1.68	1.39
12.1	k_1	87.8	32.1	17.6	13.3	10.1
	k_2	9.34	5.76	4.3	3.58	3.21
12.3	k_1	154	54.9	33.8	23.5	14
	k_2	16.4	10	7.85	6.66	5.37
12.7	k_1	425	122	78	50.5	31
	k_2	47.9	27.3	22.3	18.1	13.1
13.0	k_1	620	208	115	81.2	83.5
	k_2	73	43.2	34.2	28.4	26.4

^a k_1 and k_2 are the rate constants corresponding to the attack of OH^- ion on the substrate and half-reacted intermediate (Scheme 1). They were calculated by a computer fit of the absorbance–time data with equation (1).

Table 3. Second-order rate constants for the reaction of OH⁻ ion with *N*-ethyl-2-bromopyridinium (NEBP), compounds **I–V** (k_{12}) and their respective intermediates (k_{22})

Rate constant	Compound					
	NEBP ^a	I	II	III	IV	V
k_{12} (1 mol ⁻¹ s ⁻¹)	0.4	7.0 ± 0.8	2.6 ± 0.5	1.5 ± 0.4	1.06 ± 0.2	0.7 ± 0.1
k_{22} (1 mol ⁻¹ s ⁻¹)	—	0.8 ± 0.1	0.5 ± 0.06	0.4 ± 0.06	0.31 ± 0.04	0.25 ± 0.02

^a Second-order rate constant for the reaction of NEBP with OH⁻ from Ref. 20.

Table 4. Secondary isotope effect of D₂O on the rate of reaction of **I** with OD⁻

	k_1 (s ⁻¹)	k_2 (s ⁻¹)
NaOH/H ₂ O ^a	0.11	0.011
NaOD/D ₂ O ^a	0.13	0.013

^a [OD⁻] = [OH⁻] = 0.01 M.

excess or constant (buffer) OH⁻, k_1 and k_2 are the pseudo-first-order rate constants $k_{21}[\text{OH}^-]$ and $k_{22}[\text{OH}^-]$, respectively. The corresponding equation describing the variation of Abs with time for this reaction pathway (Scheme 1) is²⁶

$$\text{Abs} = A_0 \{ \varepsilon_c (k_2 - k_1) + e^{-k_1 t} [k_2 (\varepsilon_a - \varepsilon_c) + k_1 (\varepsilon_b - \varepsilon_a)] + e^{-k_2 t} [k_1 (\varepsilon_c - \varepsilon_b)] \} \quad (2)$$

where A_0 is the initial RPBr concentration and ε_a , ε_b and ε_c are the molar extinction coefficients of RPBr, intermediate product and final bispyridone, respectively. The fit of the experimental data to equation (1) is exemplified in Fig. 2. The formation of a 1-(2-pyridone)- ω -(bromopyridinium)alkane accounts for the single isosbestic point in Figure 1. The final product, bispyridone (Scheme 1), is formed by a slower attack of OH⁻ on the intermediate.

The isolation and characterization of the intermediate and final products (see Experimental and Table 1) demonstrate that the reaction pathway proposed in Scheme 1 adequately describes the reaction of **I–V** with OH⁻ and validates the use of a kinetic analysis using equation (2).

The pH dependence of the rate constants for the two kinetic transients (Scheme 1), obtained by computer fitting of the data using equation (2), are presented in Table 2. The slopes of the log k versus pH plots were 1.0 ± 0.02 for both k_1 and k_2 , indicating that both reactions are first order in OH⁻ ion over this pH range. The second-order rate constants for the reactions of **I–V**, and their respective intermediates, with OH⁻ (k_{12} and k_{22} , Scheme 1) are presented in Table 3. The second-order rate constant for OH⁻ attack on *N*-ethyl-2-bromopyridinium (NEBP) is included for comparison.²⁰

The moderate rate increase in both reaction steps, using OD⁻ as a nucleophile in D₂O as a solvent (Table 4), suggests that nucleophilic attack is rate limiting.²⁵

The Arrhenius plots were linear for both reaction steps from 10 to 60°C and the activation parameters, for the reactions of **I** and NEBP with OH⁻ ion, are presented in Table 5. The 10-fold difference between the rate constants for attack of OH⁻ ion on **I** and on the intermediate is due to a favorable enthalpy of activation, partially compensated for by an unfavorable activation entropy (Table 5).

Added salts decreased the reaction rate (Table 6). The extrapolated value of k_{12} to zero salt concentration (linear plot of log k_{12} against the square root of the ionic strength) was similar for NaF and NaBr. The effect of salt on the rate constant for the attack of OH⁻ on **I** is larger than that on the intermediate (Table 6). The (negative) salt effect was expected since the reaction of dipositive ions, such as **I–V**, with OH⁻ ion should be inhibited by salt and the effect should be larger for k_1 than for k_2 (Scheme 1) since only the initial substrate is a dipositive ion.²⁷

The results on the kinetic effect of bis-positive double reactive pyridinium ions are compatible with a simple

Table 5. Activation parameters for the reaction of **I** and NEBP with OH⁻ ion^a

Reaction	E_a (kcal mol ⁻¹)	ΔH^\ddagger (kcal mol ⁻¹)	ΔS^\ddagger (cal mol ⁻¹ K ⁻¹)
OH ⁻ + I ^b	12.5	11.9	-13.4
Intermediate ^c + OH ⁻	15.4	14.8	-8.1
NEBP ^d + OH ⁻	15.8	15.2	-8.3

^a NaOH = 0.01 M, [**I**] = 1.7×10^{-5} M.

^b [NaOH] = 0.01 M, [**I**] = 1.7×10^{-5} M.

^c See Scheme 1.

^d Data from Ref. 20.

Table 6. Effect of salts on the rate of reaction of **I** with OH⁻ ion

Added Salt	Concentration (M)	k_1 (s ⁻¹)	k_2 (s ⁻¹)
None	—	0.41	0.04
NaF	0.1	0.24	0.038
	0.2	0.23	0.036
	0.3	0.21	0.033
	0.4	0.18	0.033
	0.5	0.15	0.028
	1.0	0.12	0.024
NaBr	0.1	0.2	0.03
	0.2	0.14	0.027
	0.3	0.13	0.024
	0.4	0.14	0.022
	0.5	0.10	0.019
	1.0	0.087	0.016

through-space electrostatic effect when analyzed as a function of the average distance. For the short-chain compounds the value of k_{22} is still larger than that of (the reference) *N*-ethyl-substituted bromopyridinium (NEBP) (Table 3). The value of k_{22} decreases steadily with increasing distance and for compound **V** k_{22} is about half of that for NEBP (Table 3). The modest rate enhancement for OH⁻ attack on **I**, when compared with the reaction of the same nucleophile with the intermediate product, can therefore be ascribed to a through-space electrostatic effect on the reaction center. Therefore, the electrostatic effect could be due to an increase in the stability of the initial charge-transfer complex between the nucleophile and the double positive charge on the reactivity at reaction center.

CONCLUSION

We have shown that the reaction of hydroxide ion with 1, ω -bis(2-bromopyridinium)alkanes proceeds with a fast initial formation of 1-(2-pyridone)- ω -(2-bromopyridinium)alkane, followed by a slower hydroxide attack and final formation of 1, ω -bis(2-pyridone)alkane. As the number of methylene groups between the positively charged 2-bromopyridinium rings increases from three to six, the relative rates of initial attack approach that of reaction OH⁻ with 2-bromopyridinium ion. The rate enhancement, attributed to a through-space charge effect, reaches 20-fold for the propane derivative. Since a further approximation of the charged reaction centers in a

premicellar aggregate is unlikely, we suggest that the additional rate enhancement found in premicellar aggregates of comparable pyridinium rings stems from ion condensation in the aggregate.

Acknowledgments

This work was supported by the Brazilian grant agencies CNPq, FAPESP, CAPES and FINEP.

REFERENCES

1. E. M. Kosower and J. W. Patton. *Tetrahedron* **22**, 2081 (1966)
2. N. Hioka, M. J. Politi and H. Chaimovich. *Tetrahedron Lett.* **30**, 1051 (1989).
3. M. J. Politi and H. Chaimovich. *J. Phys. Org. Chem.* **4**, 207 (1991).
4. L. S. Romsted. in *Surfactants in Solution*, p. 1015. Plenum Press, New York (1984).
5. B. D. Anderson, R. A. Conradi and K. Johnson. *J. Pharm. Sci.* **72**, 448 (1983).
6. S. Scheier, A. T. Amaral, A. S. Stachissini and M. L. Bianconi. *Bull. Magn. Reson.* **8**, 166 (1986).
7. C. J. Suckling and A. A. Wilson. *J. Chem. Soc., Perkin Trans. 2* 1616 (1981).
8. S. O. Onyriuka, C. J. Suckling and A. A. Wilson. *J. Chem. Soc. Faraday. Trans. 2* 1103 (1983).
9. C. N. Sukeinik and J. K. Sutter. *J. Org. Chem.* **49**, 1295 (1984).
10. D. A. Jaeger and D. Bolikai. *J. Org. Chem.* **51**, 1350 (1986).
11. M. J. Politi, I. M. Cuccovia, H. Chaimovich, M. L. C. Almeida, J. B. S. Bonilha and F. H. Quina. *Tetrahedron Lett.* 115 (1978).
12. (a) J. H. Fendler. *Membrane Mimetic Chemistry*. Wiley, New York, (1982); (b) C. A. Bunton and G. Savelli. *Adv. Phys. Org. Chem.* **22**, 213 (1986).
13. V. R. Correia, I. M. Cuccovia, S. Stelmo and H. Chaimovich. *J. Am. Chem. Soc.* **114**, 2144 (1992).
14. P. Mukerjee, K. J. Mysels and C. I. Dulin. *J. Phys. Chem.* **62**, 1490 (1958).
15. P. Mukerjee. *J. Phys. Chem.* **62**, 1397 (1958).
16. P. Mukerjee and K. J. Mysels. *J. Phys. Chem.* **62**, 1400 (1958).
17. B. Lindman and B. Brun. *J. Colloid Interface Sci.* **42**, 388 (1973).
18. R. Friman, K. Pettersson and P. Stenius. *J. Colloid Interface Sci.* **53**, 90 (1975).
19. D. Eagland and F. Franks. *Trans. Faraday Soc.* **61**, 2468 (1965).
20. H. A. Al-Lohedan, C. A. Bunton and L. S. Romsted. *J. Org. Chem.* **47**, 3528 (1982).
21. G. B. Barlin, J. A. Benbow. *J. Chem. Soc., Perkin Trans. 2* 790 (1974)
22. Q. Schales and S. S. Schales. *J. Biol. Chem.* **140**, 879 (1941).
23. C. Fernandez. Master's Dissertation, Instituto de Química, Universidade de São Paulo (1991).
24. R. A. Zeeuw, P. E. W. Van der Laan, J. E. Greving and F. J. W. van Mansvelt. *Anal. Lett.* **9**, 831 (1976).
25. R. B. Moodie. *J. Chem. Res. (S)*, 144 (1986)
26. J. H. Espenson. *Chemical Kinetics and Reaction Mechanisms*. McGraw-Hill, New York, (1981).
27. S. W. Benson. *The Foundations of Chemical Kinetics*. McGraw-Hill New York, (1960).